Journal of Modern Optics
Publication details, including instructions for authors and subscription information:
http://www.tandfonline.com/loi/tmop20

Ultrashort pulse generation from mode-locked erbium-doped fibre ring lasers

Chir-Weei Chang [a] & Sien Chi [b]

[a] Chung Shan Institute of Science and Technology , PO Box 90008-8-10, Lung-Tan, Taiwan , 325, Republic of China

[b] Institute of Electro-Optical Engineering, National Chiao Tung University , Hsinchu, Taiwan , 300, Republic of China

Published online: 03 Jul 2009.

To cite this article: Chir-Weei Chang & Sien Chi (1999) Ultrashort pulse generation from mode-locked erbium-doped fibre ring lasers, Journal of Modern Optics, 46:9, 1431-1442

To link to this article: http://dx.doi.org/10.1080/09500349908231345

JOURNAL OF MODERN OPTICS, 1999, VOL. 46, NO. 9, 1431–1442

Ultrashort pulse generation from mode-locked erbium-doped fibre ring lasers

CHIR-WEEI CHANG

Chung Shan Institute of Science and Technology, PO Box 90008-8-10, Lung-Tan, Taiwan 325, Republic of China

and SIEN CHI

Institute of Electro-Optical Engineering, National Chiao Tung University, Hsinchu, Taiwan 300, Republic of China

(*Received 1 October 1998; revision received 6 January 1999*)

Abstract. A theoretical model of a passively mode-locked erbium-doped fibre ring laser using nonlinear polarization rotation is developed. Numerical simulations are used to study mode-locking and pulse dynamics in a typical ring configuration. The simulations show that stable operation can exist in both isotropic and birefringent fibres, and stable pulses with a FWHM as short as 45 fs can be generated. It is found that there is an optimal regime of ellipticity such that the stable mode-locking can be obtained. In addition, the condition for high birefringence approximation is also found.

1. Introduction

Passively mode-locked lasers are attractive light sources of ultrashort pulses for applications in the fields of telecommunications, sensor technology, and photonic switching. In the past few years, several kinds of mode-locked fibre lasers have been studied and developed. The phenomenon of nonlinear polarization rotation (NPR) in optical fibres has been applied to the mode-locked fibre laser for the generation of ultrashort optical pulses [1]. Recent experiments [2–5] have shown that self-starting passive mode-locking of an Er-doped fibre ring laser could be obtained through NPR and femtosecond pulses have been generated using short standard fibres [3–5]. More recently, the stretched-pulse technique combined with external chirp compensation has been employed to produce high energy ultrashort pulses [6]. Under the assumption that the pulse travelling through the laser cavity experiences only a small change by each element in the cavity, it is possible to write down a master equation of the laser that yields a closed form solution, in general a chirped secant hyperbolic in time. However, practical systems do not operate so simply and require computer simulation for accurate prediction of their behaviour. In order to achieve the shortest stable output pulses from such a laser, proper modelling of the laser becomes more critical. Besides, the details of the pulse evolution in passively mode-locked fibre ring lasers are still not very well understood. It is the purpose of this work to present a simulation model that can help us to understand and improve fibre lasers that use NPR for mode-locking. Previous modelling of the NPR fibre lasers

Journal of Modern Optics ISSN 0950–0340 print/ISSN 1362–3044 online © 1999 Taylor & Francis Ltd
http://www.tandf.co.uk/JNLS/mop.htm
http://www.taylorandfrancis.com/JNLS/mop.htm

was based on the coupled nonlinear Schrödinger equations without the coherence term [7, 8], and the influence of third-order dispersion and Raman effects were not taken into account. Theoretical results show that the coherence term, which can be neglected in highly birefringent fibre, plays an important role in low birefringence fibres [9]. This coherence term can lead to an instability in which a slow-moving partial pulse transfers energy to the fast-moving partial pulse. In practise, standard fibres usually have weak linear birefringence with beat lengths L_B around 2–10 m at 1.55 μm [2, 3]. Therefore, the coherence term should be added for an accurate description of fibre ring lasers in this case [10, 11].

In this paper we present a model for a mode-locked erbium-doped fibre laser by using NPR to fully characterize the generation of the ultrashort pulses. The model is based on the Maxwell–Bloch equations in which we have shown that solving the Bloch equations for the pumped erbium ions is equivalent to using a complex Lorentzian gain profile [12]. Also, we have considered third-order dispersion, cross-Raman effects and coherent coupling for the ultrashort pulses. In the stable operation region, although the third-order dispersion and Raman effects often have little qualitative effect on the system, a detailed quantitative analysis for fibre ring lasers should consider these effects [11]. We have shown with this model that the stable output pulses can be generated from a mode-locked fibre ring laser with an isotropic fibre, and how the output pulse behaviour is affected by the initial polarization state of the field and the linear birefringence of the fibre. Although real fibres always have some linear birefringence, as mentioned before, the isotropic model still offers important qualitative insight on the system operation. At the limit where the induced nonlinear birefringence dominates any linear birefringence, the fibre can be considered isotropic. It is therefore important to understand pulse evolution in isotropic, non-birefringent fibres. The model can be used to optimize cavity design by searching through a range of parameters in order to generate stable short pulses from fibre ring lasers. The stability analysis and optimization of pulse ellipticity may be important in other practical applications as well. These include logic gates, intensity discriminators and the Kerr shutter.

2. Theoretical model

2.1. *Pulse evolution equations*

Following our earlier work on soliton pulse train amplification [13], we describe the gain in an erbium-doped fibre amplifier by a complex Lorentzian gain profile, which includes the effect of gain saturation and pump absorption. The coupled modified nonlinear Schrödinger equations describing femtosecond-range pulse propagation in a linearly birefringent erbium-doped fibre are [13, 14]

$$\mathrm{i}\frac{\partial u}{\partial \xi}+\kappa u+\mathrm{i}\delta\frac{\partial u}{\partial \tau}+\frac{1}{2}\frac{\partial^2 u}{\partial \tau^2}-\mathrm{i}d\frac{\partial^3 u}{\partial \tau^3}+|u|^2u+\tfrac{2}{3}|v|^2u+\tfrac{1}{3}v^2u^*$$
$$-\left(c_1u\frac{\partial |u|^2}{\partial \tau}+c_2u\frac{\partial |v|^2}{\partial \tau}+c_3v\frac{\partial uv^*}{\partial \tau}\right)$$
$$=\frac{1}{4\pi}\Gamma_0\int_{-\infty}^{\infty}[f(\omega-\omega_0)+\mathrm{i}g(\omega-\omega_0)]\,\tilde{u}(\xi,\omega)\,\exp(-\mathrm{i}\omega t)\,\mathrm{d}\omega, \quad (1\,a)$$

$$i\frac{\partial v}{\partial \xi} - \kappa v - i\delta\frac{\partial v}{\partial \tau} + \frac{1}{2}\frac{\partial^2 v}{\partial \tau^2} - id\frac{\partial^3 v}{\partial \tau^3} + |v|^2 v + \tfrac{2}{3}|u|^2 v + \tfrac{1}{3}u^2 v^*$$
$$-\left(c_1 v\frac{\partial |v|^2}{\partial \tau} + c_2 v\frac{\partial |u|^2}{\partial \tau} + c_3 u\frac{\partial u^* v}{\partial \tau}\right)$$
$$= \frac{1}{4\pi}\Gamma_0 \int_{-\infty}^{\infty} [f(\omega-\omega_0) + ig(\omega-\omega_0)]\,\tilde{v}(\xi,\omega)\exp(-i\omega t)\,d\omega, \quad (1b)$$

where

$$f(\omega-\omega_0) = \frac{-(\omega-\omega_0)T_2}{1+(\omega-\omega_0)^2 T_2^2}, \qquad g(\omega-\omega_0) = \frac{1}{1+(\omega-\omega_0)^2 T_2^2},$$
$$\Gamma_0 = \frac{T_0^2}{|\beta_2|}\sigma_s W_{ss}(\xi).$$

In equation (1), u and v are the normalized field components of the slow and fast axes, respectively (when δ is positive), 2κ is the normalized wavenumber difference, 2δ is the corresponding inverse group velocity difference, d is the normalized third-order dispersion parameter, ξ is the normalized distance, and τ is the normalized time. The terms with factors of 2/3 represent the effect of cross-phase modulation. The effect of coherent coupling is represented by the terms with factors of 1/3. The terms within parentheses represent the Raman effect in a birefringent fibre. Both the parallel and perpendicular Raman effects are retained in these equations, where $c_1 = T_R/T_0$ and $c_2 = c_3 = c_1/3$. Here $T_0 = T_{FWHM}/1.763$ is the normalized pulse width and the Raman coefficient T_R is assumed to be 3 fs in our simulations. The lineshape functions $f(\omega-\omega_0)$ and $g(\omega-\omega_0)$ represent dopant-induced dispersion and gain profiles, respectively, where ω_0 is the carrier frequency of the signal pulse and T_2 is the polarization relaxation time of the pumped erbium ions. Γ_0 is the normalized peak gain coefficient and $\Gamma_0 = 0$ is the passive fibre, where β_2 is the group velocity dispersion parameter, σ_s is the emission cross-section at the signal wavelength, and $W_{ss}(\xi)$ is the steady-state solution of the population inversion. The terms with coefficient κ can be eliminated by ξ dependent phase transformations of u and v. This in turn gives the nonlinear terms with coefficient 1/3 rapid phase variations with ξ which allows them to be neglected in the case of highly birefringent fibres. However, a phase shift between u and v alters the state of polarization of the field, so it is more convenient to use the form of equations (1).

2.2. *Gain saturation and pump absorption*

Since the depletion of the population inversion by a single pulse is negligible, the gain saturation can be described by the averaged power of the signal pulse train, and the steady-state solution $W_{ss}(\xi)$ can thus be obtained by solving the three-level rate equation:

$$W_{ss}(\xi) = \frac{\bar{I}_p(\xi) - 1}{1 + \bar{I}_p(\xi) + \bar{I}_s(\xi)} N_0, \quad (2)$$

where

$$\bar{I}_p = \frac{\sigma_p I_p T_1}{h\nu_p}, \qquad \bar{I}_s = \frac{2\sigma_s I_s T_1}{h\nu_s}.$$

In equation (2), I_p and I_s are the intensities of the pump and signal beams, respectively; $h\nu_p$ and $h\nu_s$ are the photon energies of the pump and signal waves, respectively; σ_p is the absorption cross-section at the pump wavelength; N_0 is the doping density of the erbium ions, and T_1 is the relaxation time of the population inversion. The equation describing the evolution of the pump intensity is

$$\frac{1}{I_p(\xi)}\frac{dI_p(\xi)}{d\xi} = -\sigma_p N_1(\xi) - \alpha_p, \tag{3}$$

where

$$N_1(\xi) = \frac{1 + 0.5\bar{I}_s(\xi)}{1 + \bar{I}_p(\xi) + \bar{I}_s(\xi)} N_0.$$

In equation (3), N_1 is the steady-state population density of the lower laser level, and α_p is the intrinsic fibre loss at the pump wavelength. It is worth mentioning that the effect of pump absorption plays an important role in the phenomenon of gain saturation and cannot be ignored.

2.3. *Modelling of polarization controllers*

Figure 1 is a schematic diagram of the mode-locked fibre ring laser to be considered. The ring laser consists of an erbium-doped fibre section, two polarization controllers, and a Faraday (polarization-sensitive) isolator. The Faraday isolator plays the dual role of an isolator that forces unidirectional operation and a polarizer such that light leaving the isolator is linearly polarized. In our analysis, the isolator consisted of an input polarizer and an output polarizer rotated by 45° relative to each other. To achieve the mode-locking effect, fibre ring lasers usually have two polarization controllers. The first controller (PC 1) changes the polariza-

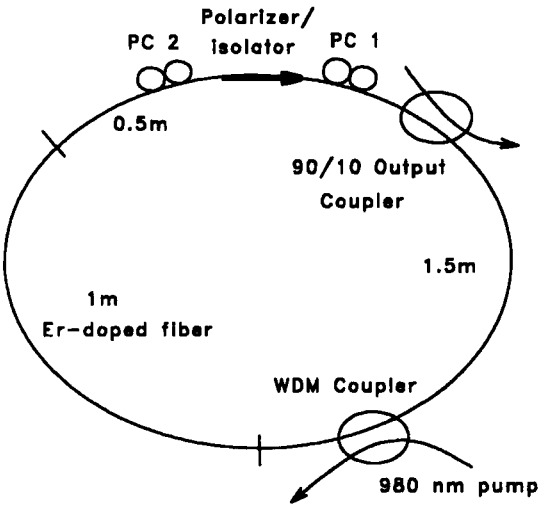

Figure 1. Schematic diagram of the fibre laser cavity. The ring cavity of this laser incorporated 1 m of erbium-doped fibre with a total length of 3 m.

tion state from linear to elliptical and the second (PC 2) biases the system to a point where higher intensities experience lower loss.

The polarization controller is modelled by a polarization transformation matrix **P**, which can be represented by the product of three matrices

$$\mathbf{P} = \begin{bmatrix} \cos\psi & -\sin\psi \\ \sin\psi & \cos\psi \end{bmatrix} \begin{bmatrix} \exp(-i\Gamma/2) & 0 \\ 0 & \exp(i\Gamma/2) \end{bmatrix} \begin{bmatrix} \cos\psi & \sin\psi \\ -\sin\psi & \cos\psi \end{bmatrix},$$

where Γ and ψ are the phase retardation and azimuth angle, respectively. After passing through the first controller, an elliptical polarization state is obtained. The state of polarization can be described by the ellipticity $\epsilon = b/a$ defined as the ratio of the major to minor axis of the polarization ellipse and the angle Φ, which is the angle between the ellipse major axis and the slow axis of the fibre. a, b and Φ are given by

$$a^2 = |u|^2 \cos^2\Phi + |v|^2 \sin^2\Phi + 2|u||v| \cos\delta \cos\Phi \sin\Phi, \tag{4a}$$

$$b^2 = |u|^2 \sin^2\Phi + |v|^2 \cos^2\Phi - 2|u||v| \cos\delta \cos\Phi \sin\Phi, \tag{4b}$$

$$\tan(2\Phi) = \frac{2|u||v|}{|u|^2 - |v|^2} \cos\delta, \tag{4c}$$

where δ is the phase difference between u and v. For simplicity and without loss of generality we assume that the first controller is aligned along the slow axis of the fibre; i.e. $\psi_1 = 0$ was assumed. In this case, the initial ellipticity ϵ and ellipse angle Φ of the polarization can then be expressed as follows:

$$\epsilon^2 = \frac{\sin^2(\theta_E - \Phi) + \sin(2\theta_E) \sin(2\Phi) \sin^2(\Gamma_1/2)}{\cos^2(\theta_E - \Phi) - \sin(2\theta_E) \sin(2\Phi) \sin^2(\Gamma_1/2)}, \tag{5a}$$

$$\tan(2\Phi) = \tan(2\theta_E) \cos\Gamma_1, \tag{5b}$$

where Γ_1 is the phase retardation of PC 1, $\theta_E \equiv \theta + \pi/4$ is the angle between the polarization axis of the output polarizer of the isolator and the slow axis, and the angle of the input polarizer of the isolator is assumed to be θ.

The second controller is then adjusted in such a way that there will be no transmission for low-power light; i.e. after passing through the second controller, the state of polarization of the low-power portion is linear and orthogonal to the polarization axis of the input polarizer of the isolator. In this case

$$\mathbf{P} \begin{bmatrix} |u_L| \\ |v_L| \exp(i\delta_L) \end{bmatrix} = (|u_L|^2 + |v_L|^2)^{1/2} \begin{bmatrix} \cos\left(\theta + \frac{\pi}{2}\right) \\ \sin\left(\theta + \frac{\pi}{2}\right) \end{bmatrix} \exp(i\phi), \tag{6}$$

where u_L and v_L are the amplitudes of the low-power components of u and v, which experience only linear effects when propagating in the fibres, δ_L is the phase difference between u_L and v_L, and ϕ is a parameter that represents the common phase shift of the two components. Equation (6) can be solved to obtain the phase retardation Γ_2 and azimuth angle ψ_2 of the PC 2 as follows:

$$\tan(2\psi_2) = \frac{|v_L|^2 - |u_L|^2 \cot^2\theta}{\cot\theta(|u_L|^2 + |v_L|^2) + |u_L||v_L|\cos\delta_L(1+\cot^2\theta)}, \tag{7a}$$

$$\tan\left(\frac{\Gamma_2}{2}\right) = \frac{|v_L|\cos\delta_L + |u_L|\cot\theta}{|v_L|\sin\delta_L[\cos(2\psi_2) - \cot\theta\sin(2\psi_2)]}. \tag{7b}$$

The polarization mode amplitudes after passing through the controller can be obtained by

$$\begin{bmatrix} u' \\ v' \end{bmatrix} = \mathbf{P}\begin{bmatrix} u \\ v \end{bmatrix}, \tag{8}$$

where Γ_2 and ψ_2 within the polarization transfomation matrix $\mathbf{P}$ are determined by equation (7).

3. Numerical results and discussion

The typical parameters used to solve equations (1)–(3) numerically are as follows: signal wavelength, 1.53 μm; pump wavelength, 0.98 μm; $\beta_2 = -4\,\mathrm{ps^2\,km^{-1}}$; $\beta_3 = 0.1\,\mathrm{ps^3\,km^{-1}}$; $T_2 = 0.1$ ps; $T_1 = 11.5$ ms; $T_R = 3$ fs; $\sigma_s = 7.75 \times 10^{-25}\,\mathrm{m^2}$; $\sigma_p = 3.12 \times 10^{-25}\,\mathrm{m^2}$; $\alpha_p = 1.0\,\mathrm{dB\,km^{-1}}$; $N_0 = 1.34 \times 10^{19}\,\mathrm{ions\,cm^{-3}}$, which corresponds to 1300 ppm doping density, and pump power = 80 mW. Equation (1) is solved by using the split-step Fourier method assuming the initial condition

$$u(\xi = 0, \tau) = A\,\mathrm{sech}(\tau)\cos\theta_E, \tag{9a}$$

$$v(\xi = 0, \tau) = A\,\mathrm{sech}(\tau)\sin\theta_E, \tag{9b}$$

which is a linearly polarized pulse injected into the fibre right behind the output polarizer of the isolator at amplitude A and input polarization angle $\theta + \pi/4(\equiv \theta_E)$ with respect to the u axis. By using an input seed pulse with relatively low amplitude which represents the initial noise disturbance, self-starting is possible provided that doping density and pump power are high enough. Stable operation regimes for a certain range of parameters have been found. Also, the final steady-state pulse is independent of the amplitude and width of the initial injected pulse.

3.1. *Mode-locking using an isotropic fibre*

In an isotropic Kerr medium, there will be no polarization change if the incident light is linearly polarized. As the field passes through the isolator in figure 1, the linearly polarized light is produced. Therefore, without PC 1, there is no nonlinear polarization rotation in the isotropic fibre. Thus it is important to find the initial polarization state of the light such that stable operation can be achieved. In the isotropic case, the ellipse angle Φ is defined as the angle between the ellipse major axis and the slow axis of PC 1 ($\psi_1 = 0$).

In our numerical simulations, we have found that the stability of the pulsed output greatly depends on the value of ellipticity ϵ. In figure 2, we show this character as a function of the initial polarization state of different angles θ for injected pulses with FWHM = 1 ps and $A = 0.1$. For each curve, the phase retardation Γ_1 is varied from 0–90° and the state of polarization is obtained from equation (5). Solid lines show the stable operation regimes. For operating points

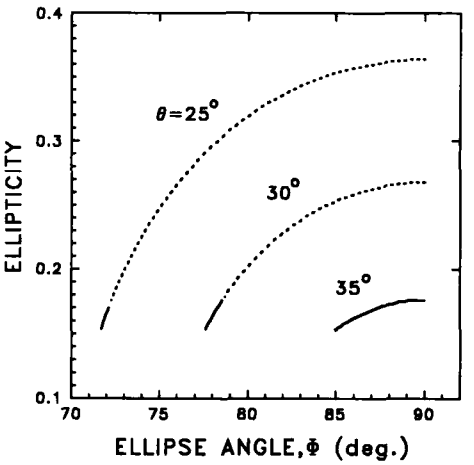

Figure 2. The stability of the laser output as a function of the initial polarization state at different isolator angles θ. Solid lines show the stable mode-locking regimes. Dashed curves denote the output was either periodic (with period greater than one cavity round trip time) or chaotic.

below the solid lines, the signal power level decreases continuously from round to round. Dashed curves in figure 2 indicate the output was either periodic (with period greater than one cavity round trip time) or chaotic, which corresponds to unstable operating conditions.

The reason can be understood by noting that in the early stages of pulse formation, the intensity-induced transmission at the isolator increases as the ellipticity increases. Thus it is obvious that large ellipticity provides a much larger transmission. In the small ellipticity regime ($\epsilon \sim 0$), nonlinear transmission is low and there is no pulsed output. Once the nonlinear transmission exceeds a threshold value, the output is stable pulses. As the nonlinear transmission increases, a bifurcation point is reached. Beyond the first bifurcation the output of the ring laser alternates between two pulses of clearly distinct energy levels, which has been observed experimentally [15–17]. As the nonlinear transmission increases further, the output pulse train will be characterized by sequences of increasing period. Eventually, when the nonlinear transmission of the system becomes sufficiently large, the pulse evolution shows a random character. This scenario is referred to as the period doubling route to chaos, which happens rather frequently in nonlinear dynamics systems.

Figure 2 clearly shows that there is an optimal regime of the initial ellipticity such that the intensity-induced ellipse rotation is particularly efficient for stable operation, and the stable mode-locking could be obtained only for the ellipticity parameter ϵ ranging from 0.15 to 0.18. Although the pulse formation is sensitive to the various system parameters, it is difficult to determine the optimum values to be used in the simulation. In our numerical studies for other cases we find that the stable output pulses can be generally obtained with ϵ between 0.10–0.25.

Figure 3 shows the evolution of the stable output pulse with initial ellipticity $\epsilon = 0.16$ and ellipse angle $\Phi = 71.9°$ through forty round trips. The result is a stable pulse train of width 50 fs that is free of pedestal. The minimum stable pulse width obtained in our simulations is around 45 fs for the operating points near to the first bifurcation point.

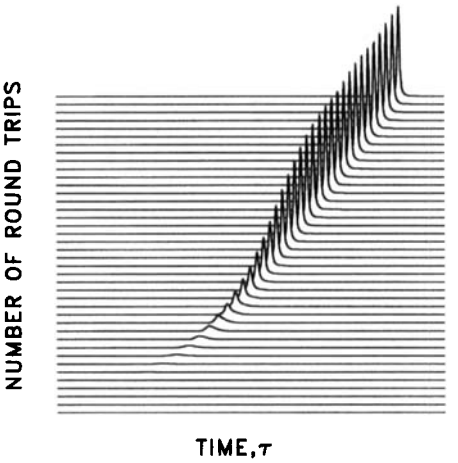

Figure 3. Evolution of the stable output pulse (FWHM = 50 fs) with initial ellipticity $\epsilon = 0.16$ and ellipse angle $\Phi = 71.9°$.

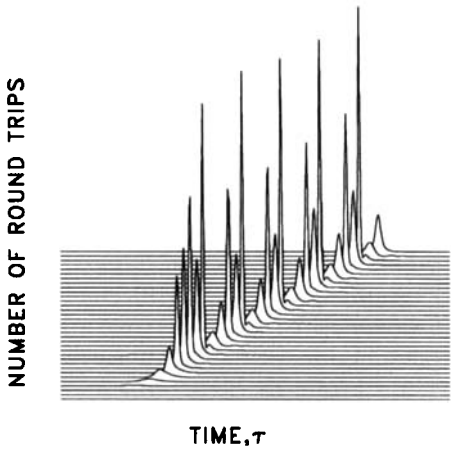

Figure 4. Evolution of a period-5 output state with initial ellipticity $\epsilon = 0.24$ and ellipse angle $\Phi = 74.7°$.

Figure 4 shows the evolution of a period-5 state with initial ellipticity $\epsilon = 0.24$ and ellipse angle $\Phi = 74.7°$. The result is characterized by five distinct pulses that alternate with one another at the output of the ring cavity. If the intensity-induced transmission at the isolator increases further, the system enters the chaotic regime. An example is illustrated in figure 5, where the input polarization state has the ellipticity $\epsilon = 0.29$ and ellipse angle $\Phi = 77.2°$.

When an elliptically polarized pulse travels through the fibre, the ellipse angle Φ at the peak intensity of the pulse can be calculated according to equation (4), and the polarization ellipse was observed to rotate between 15° and 25° in the case of stable operation. This verifies that the mode-locking is sustained by NPR. A typical result is shown in figure 6, where $\Delta\Phi_M$ and $\Delta\Phi_E$ denote the angles rotated by the polarization ellipse at the middle and end points in the cavity, respectively. The corresponding pulse evolution is shown in figure 3. As can be seen, $\Delta\Phi_E$ is much larger than $\Delta\Phi_M$ because of the rate of ellipse rotation is intensity dependent.

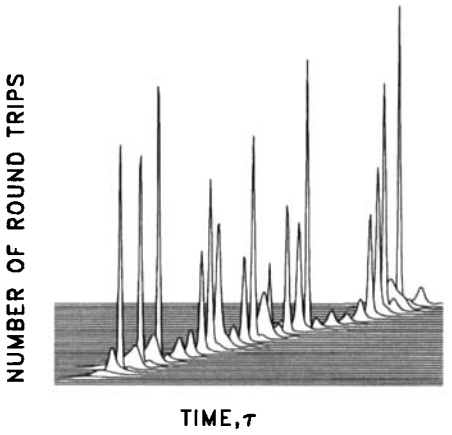

Figure 5. Evolution of a chaotic output state with initial ellipticity $\epsilon = 0.29$ and ellipse angle $\Phi = 77.2°$.

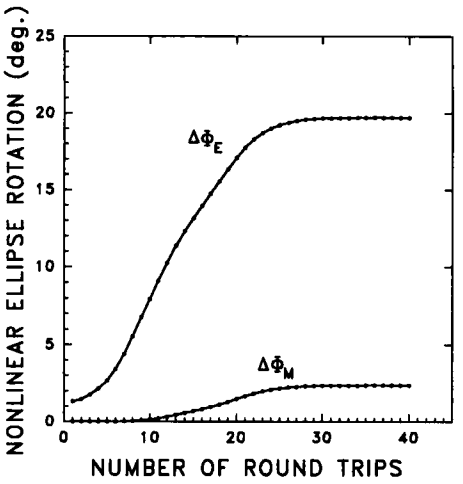

Figure 6. Ellipse rotation of the laser pulse as a function of the number of cavity round trips at the middle ($\Delta\Phi_M$) and end ($\Delta\Phi_E$) points in the cavity. The corresponding pulse evolution is shown in figure 3.

It should be noted that, owing to the complexity of the problem and the number of parameters involved, the numerical studies could not be exhaustive. We investigate theoretically only the nonlinear pulse dynamics and therefore environmental perturbations and other uncontrollable effects may be neglected. However, our simulation results show that the instability due to the sideband generation of a periodically perturbed soliton is practically unavoidable, whenever high pump power and heavy doping density are used.

3.2. *Mode-locking using an birefringent fibre*

If a birefringent fibre is used in figure 1, linear and induced nonlinear birefringence coupling with each other takes place, and it is important to take into account their interplay. In our simulations, we note that both the range and the output pulse power of stable operation are strongly affected by the linear

birefringence. We have found that the output pulse width and peak power were significantly affected by the strength of the birefringence. In general, the output pulse power shows an oscillation variation with varied periods as the birefringence is changed continuously [11].

In order to check the validity of the isotropic approximation, very weakly birefringent fibres are used in figure 1. As shown in figure 7, the solid curve shows the pulse shape at stable output of the ring laser after thirty round trips with beat lengths $L_B = 200\,\text{m}$, initial ellipticity $\epsilon = 0.17$ and ellipse angle $\Phi = 78.1°$. For comparison, the result obtained from the isotropic model is shown by the dashed curve, where the linear birefringence was neglected in equation (1). On the other hand, when highly birefringent fibres are used in figure 1, our numerical results show that the approximation of high birefringence is valid for $L_B \leq 0.1\,\text{m}$, where the effect of the coherence term is negligible. Figure 8 shows the stable output

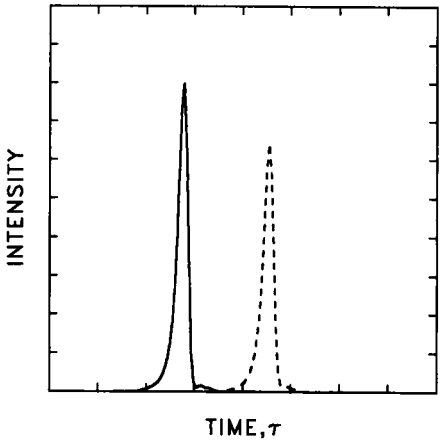

Figure 7. Pulse shape at the output of the ring laser after thirty round trips with beat lengths $L_B = 200\text{m}$, initial ellipticity $\epsilon = 0.17$ and ellipse angle $\Phi = 78.1°$. For comparison, the dashed curve shows the result obtained from the isotropic model.

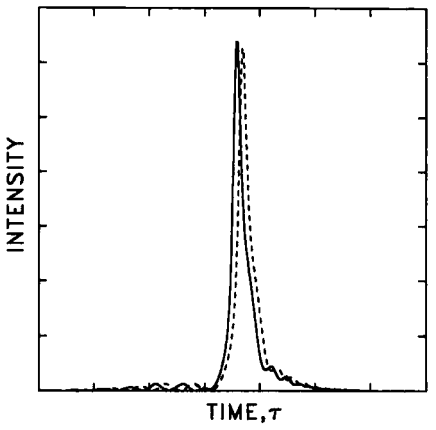

Figure 8. Output pulse shapes with (solid curve) and without (dashed curve) the coherence term in equation (1) for the case of $L_B = 0.15\,\text{m}$.

pulse shapes with (solid curve) and without (dashed curve) the coherence term in equation (1) for the case of $L_B = 0.15\,m$.

It is important to note that the linear birefringence-induced phase difference may be compensated by a polarization transformer [18], however the linear birefringence contributions to the coupling effect on the coherence term cannot be ignored [9]. Our general conclusion is that the coherence term in equation (1) should be take into account when weakly birefringent fibres are used.

4. Conclusions

In conclusion, a complete theoretical model has been developed to study the pulse-forming processes in erbium-doped fibre ring lasers and its limitations. This model can help us to understand fibre lasers that use nonlinear polarization rotation for mode-locking, and allows for a detailed analysis of the pulse dynamics in femtosecond fibre ring lasers. In particular, stable pulse parameters are determined and instability issues are discussed. Our analysis provides insight into the basic processes and mechanisms which impose a limit on the shortest pulse widths obtainable from passively mode-locked fibre ring lasers. Our numerical results verified that the pulse formation is governed by the intensity-induced polarization evolution. Numerical simulations show that stable operation can exist in both isotropic and birefringent fibres. Various operation regimes of the laser are found, and stable pulses with a FWHM as short as 45 fs can be generated. It is also shown that the effect of mode-locking can be particularly efficient and stable if the initial state of polarization is suitably chosen. Simulations show that the effects of the weak intrinsic birefringence and coherent coupling plays an important role in the pulse dynamics whenever a short standard fibre is used, and the output pulse power depends greatly on the weak linear birefringence. Also, the numerical results show that the approximation of high birefringence is valid for a beat length $\leq 0.1\,m$, where the effect of the coherent oscillating term is negligible.

References

[1] Hofer, M., Fermann, M. E., Haberl, F., Ober, M. H., and Schmidt, A. J., 1991, *Optics Lett.*, **16,** 502.
[2] Matsas, V. J., Newson, T. P., Richardson, D. J., and Payne, D. N., 1992, *Electron. Lett.*, **28,** 1391.
[3] Tamura, K., Haus, H. A., and Ippen, E. P., 1992, *Electron. Lett.*, **28,** 2226.
[4] Pandit, N., Noske, D. U., and Taylor, J. R., 1994, *J. mod. Optics*, **41,** 11.
[5] Yoshida, E., Kimura, Y., and Nakazawa, M., 1994, *Jpn. J. appl. Phys.*, **33,** 5779.
[6] Nelson, L. E., Jones, D. J., Tamura, K., Haus, H. A., and Ippen, E. P., 1997, *Appl. Phys.* B, **65,** 277.
[7] Chen, C. J., Wai, P. K. A., and Menyuk, C. R., 1992, *Optics Lett.*, **17,** 417.
[8] Afanasjev, V. V., and Grudinin, A. B., 1993, *Sov. Lightwave Commun.*, **3,** 77.
[9] Winful, H. G., 1985, *Appl. Phys. Lett.*, **47,** 213.
[10] Chang, C. W., and Chi, S., 1997, *Optics Commun.*, **134,** 218.
[11] Chang, C. W., and Chi, S., 1998, *J. mod. Optics*, **45,** 355.
[12] Chi, S., Chang, C. W., and Wen, S., 1994, *Optics Commun.*, **106,** 193.
[13] Chi, S., Chang, C. W., and Wen, S., 1994, *Optics Commun.*, **111,** 132.
[14] Evangelides, S. G., Jr, Mollenauer, L. F., Gordon, J. P., and Bergano, N. S., 1992, *J. Lightwave Technol.*, **10,** 28.

[15] BOUDEC, P. LE., JAOUEN, C., FRANCOIS, P. L., BAYON, J. F., SANCHEZ, F., BESNARD, P., and STEPHAN, G., 1993, *Optics Lett.*, **18**, 1890.
[16] LACOT, E., STOECKEL, F., and CHENEVIER, M., 1994, *Phys. Rev.* A, **49**, 3997.
[17] TAMURA, K., DOERR, C. R., HAUS, H. A., and IPPEN, E. P., 1994, *IEEE Photonics Technol. Lett.*, **6**, 697.
[18] STOLEN, R. H., BOTINEAU, J., and ASHKIN, A., 1982, *Optics Lett.*, **7**, 512.